26th International Congress on Sound and Vibration
7-11 July 2019, Montreal

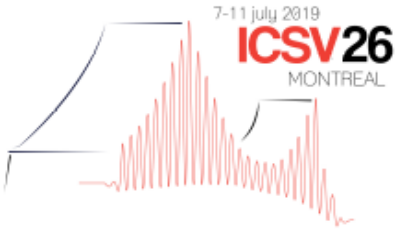

APPLICATION OF TIME-WARPING TRANSFORM FOR SEPARATION OF ACOUSTIC NORMAL MODES IN HORIZONTALLY INHOMOGENEOUS WAVEGUIDES

Oleg A. Godin and Tsu Wei Tan
Naval Postgraduate School, Monterey, CA 93943, USA
email: oagodin@nps.edu

Boris G. Katsnelson
University of Haifa, Haifa, Israel

Time-warping transform is often used in underwater acoustics to separate normal mode components of a broadband signal recorded by a single hydrophone. An important application of time warping is retrieval of modal dispersion curves for subsequent inversion of the measured mode dispersion for unknown geoacoustic parameters. The time-warping transform was developed for range-independent shallow-water waveguides. Physical parameters of the ocean are never quite constant in the horizontal plane, with bathymetry variations being typically responsible for the bulk of the waveguide's range dependence as well as horizontal refraction of sound in the coastal ocean. We use simple, exactly solvable models of shallow-water waveguides to illustrate the effects that the range dependence and horizontal refraction have on the performance of the warping transform and the inferred geoacoustic parameters. Horizontal refraction due to generic bathymetric variations is addressed in the adiabatic approximation using perturbation techniques. Theoretical predictions are verified using numerical simulations. It is found that moderate bottom slopes can lead to large errors in retrieved geoacoustic parameters and cause positive bias in bottom sound speed estimates if horizontal refraction is ignored.
Keywords: underwater acoustics, shallow-water waveguides

1. Introduction

Successful applications of a time-warping transform to retrieve normal mode dispersion curves from single-hydrophone measurements of the acoustic field due to a broadband compact sound source [1–3] or from two-point cross-correlation functions of diffuse noise [4] have reinvigorated investigations of normal mode propagation in the coastal ocean and sensitivity of the dispersion curves to various environmental parameters. The time-warping transform was originally developed for range-independent waveguides, and the retrieved normal mode travel times are usually inverted for unknown geoacoustic parameters or sound source coordinates assuming a range-independent ocean. This paper investigates theoretically the effects that seafloor slope has on the normal mode dispersion and time warping, and the errors that emerge from neglecting horizontal inhomogeneity of the ocean when interpreting time-warping results.

2. Theory

2.1 Simple waveguides

Introduce a Cartesian coordinate system with horizontal coordinates x and y and a vertical coordinate z. A homogeneous fluid layer with sound speed c and density ρ is located between plane boundaries $z = 0$ and $z = H$ with normal impedances Z_0 and Z_H, respectively. By imposing the boundary conditions of impedance continuity at $z = 0$ and $z = H$ on the solution of 1-D wave equation in the homogeneous fluid layer, we obtain the dispersion relation

$$\tan\left(\omega H\sqrt{c^{-2}-c_n^{-2}}\right)=i\rho_w\sqrt{c^{-2}-c_n^{-2}}\,\frac{Z_0+Z_H}{\rho_w^2+\left(c^{-2}-c_n^{-2}\right)Z_0Z_H} \tag{1}$$

of the acoustic normal modes supported by the waveguide. Here c_n is the phase speed of n-th normal mode, $n = 1, 2, \ldots$.

Let the impedances depend only on the angle of incidence of a plane wave (or, equivalently, on c_n) and be independent of frequency. Then, wave frequency enters the dispersion equation (1) only in combination ωH. We will refer to such media as simple waveguides, for brevity. Examples of simple waveguides include a layer of fluid with pressure-release and rigid boundaries, a layer with a pressure-release boundary $z = 0$ and a homogeneous fluid half-space at $z > H$ (Pekeris waveguide), a fluid layer between a pressure release or rigid boundary and a homogeneous solid half-space at $z > H$, etc. Using well-known input impedances of fluid and solid half-spaces [5], it is straightforward to check that Eq. (1) reduces to previously established normal mode dispersion relations (see, e.g., [6]) in these special cases.

2.2 Travel times of adiabatic normal modes in range-dependent waveguides

Consider downslope underwater sound propagation in a coastal wedge. Horizontal coordinates x and y are chosen to be, respectively, perpendicular and parallel to the straight coastline. Water depth $H(x)$ increases linearly with increasing x. In the adiabatic approximation, travel time of n-th normal mode is

$$T_n=\int\frac{dx}{u_n}=\cot\alpha\int_{H_1}^{H_2}\frac{dH}{u_n\left(\omega,H\right)}. \tag{2}$$

Here H_1 and H_2 are the water depths at the source and receiver locations, $H_1 < H_2$; α is the angle that the seafloor makes with the horizontal plane; and $u_n(\omega, H)$ is the group speed of the local normal mode. It can be calculated as

$$u_n=\left(\frac{\partial}{\partial\omega}\frac{\omega}{c_n}\right)^{-1}=c_n\left(1-\frac{\omega}{c_n}\frac{\partial c_n}{\partial\omega}\right)^{-1} \tag{3}$$

from the dispersion relation of a corresponding range-independent waveguide. At upslope propagation, mode travel time is again given by Eq. (2), where H_1 and H_2 are now the receiver and source depths, respectively.

In the simple waveguides as defined in Section 2.1, mode travel time (2) can be calculated in a closed form. Since the phase speed c_n depends on ω and H only via the combination ωH, it follows from Eq. (3) that

$$\frac{1}{u_n}=\frac{1}{c_n}+\omega\left(\frac{\partial}{\partial\omega}\frac{1}{c_n}\right)_H=\frac{1}{c_n}+\omega H\frac{d}{d\left(\omega H\right)}\frac{1}{c_n}=\frac{1}{c_n}+H\left(\frac{\partial}{\partial H}\frac{1}{c_n}\right)_\omega=\left(\frac{\partial}{\partial H}\frac{H}{c_n}\right)_\omega. \tag{4}$$

Substitution of the right-most side in Eq. (4) for $1/u_n$ in Eq. (2) gives a remarkably simple result:

$$T_n = \left[\frac{H_2}{c_n(\omega, H_2)} - \frac{H_1}{c_n(\omega, H_1)} \right] \cot\alpha. \quad (5)$$

It is straightforward to extend this result to a more complicated bathymetry, where water depth is piece-wise linear function of x. Then, mode travel time is given by the sum of contributions Eq. (5) in each segment with a constant bottom slope, the slope α being different in each segment.

In the particular case of a wedge with ideal (pressure release and/or rigid boundaries) the dispersion relation (1) gives the well-known expressions

$$c_n = c\left(1 - F_n^2 f^{-2}\right)^{-1/2}, \quad u_n = c^2/c_n, \quad F_n = (n-\beta)c/2H, \quad n = 1, 2, \ldots \quad (6)$$

for the phase and group speeds. Here F_n is the cutoff frequency of n-th normal mode, $\beta = 0$ if both boundaries are pressure release or rigid and $\beta = 0.5$ if one boundary is pressure-release and the other is rigid. Using Eq. (6), it is easy to integrate over H in Eq. (2) and verify validity of Eq. (5) in this particular case.

At upslope propagation in a waveguide with ideal boundaries, the group speed (6) turns to zero at the mode cutoff. Nevertheless, the mode travel time to the mode's cutoff is finite in the wedge:

$$T_n = H_2 \cot\alpha / c_n(\omega, H_2) \quad (7)$$

according to Eq. (5). If a source and a receiver are located at points (x_1, y, z_1) and (x_2, y, z_2) and the smaller of water depths $H_1 = H(x_1)$ and $H_2 = H(x_2)$ is larger than the depth at the cutoff of n-th normal mode, there will be two arrivals of the mode. One arrival corresponds to a direct, up- or downslope path. The travel time for this arrival is given by Eq. (5). On the other path, normal mode first propagates from the source upslope to its cutoff, is totally reflected there (see, e.g., [6]), and then propagates downslope to the receiver. According to Eqs. (5) and (6), the travel time on the reflected path is

$$T_n = \left[\frac{H_2}{c_n(\omega, H_2)} + \frac{H_1}{c_n(\omega, H_1)} \right] \cot\alpha. \quad (8)$$

Up- and downslope propagation in a wedge with either fluid or solid penetrable bottom can be analysed in a similar fashion. In particular, when the bottom is a fluid with sound speed $c_b > c$, phase and group speeds at mode cutoff equal c_b [6]. Using dispersion relation (1) to determine the water depth at the n-th mode cutoff and applying Eq. (5), we find mode travel time to its cutoff from a source at (x_2, y, z_2):

$$T_n = \left[\frac{H_2}{c_n(\omega, H_2)} - \frac{(2n-1)\pi}{2\omega\sqrt{c_b^2 c^{-2} - 1}} \right] \cot\alpha. \quad (9)$$

This result reduces to Eq. (7) in the limit $c_b \to \infty$, as expected.

2.3 Horizontal refraction in an ideal wedge

Consider travel time of an adiabatic normal mode along a horizontal (modal) ray in a wedge with pressure-release and/or rigid boundaries. Let depth increase with distance x from the coastline $x = 0$: $H(x) = x \cot\alpha$. In this coordinate system, waveguide parameters are independent of y. Hence, the y-component of the wave vector $(k_x, k_y, 0)$ of the mode is constant along the modal ray (see, e.g., [6, 7]). The x-component of the wave vector increases with x on the modal ray. If $k_x > 0$ at the source, the mode propagates towards increasing x, i.e., deeper water. If $k_x < 0$ at the source, the mode propagates towards the coast line, reaches a turning point, where $k_x = 0$, and then propagates towards deeper water. The turning point

occurs at such depth H_t that $k_y = \omega/c_n(\omega, H_t)$. At upslope propagation, $k_y = 0$, and the turning point coincides with the mode's cutoff.

Let l stand for arc length along a modal ray. Then modal travel time along the modal ray is

$$T_n = \int \frac{dl}{u_n} = \int \frac{\sqrt{k_x^2 + k_y^2}}{k_x} \frac{dx}{u_n} = \cot\alpha \int \frac{\sqrt{k_x^2 + k_y^2}}{k_x} \frac{dH}{u_n}. \tag{10}$$

Taking into account that $k_x^2 + k_y^2 = \omega^2/c_n^2$ and using Eq. (6), from Eq. (10) we find an explicit equation for the mode travel time:

$$T_n = \frac{\left| \sqrt{\left(1 - \cos^2\gamma_n \sin^2\psi\right) H_r^2 - H_s^2 \sin^2\gamma_n} \mp H_s \cos\gamma_n \left|\cos\psi\right| \right|}{\left(1 - \cos^2\gamma_n \sin^2\psi\right) c \tan\alpha}. \tag{11}$$

Here H_s and H_r are water depths at the source and receiver locations, ψ is the angle the mode's wave vector makes with the positive direction of the x coordinate axis at the source, and

$$\gamma_n = \arcsin\frac{(n-\beta)c}{2fH_s} = \arccos\frac{c}{c_n(\omega, H_s)}. \tag{12}$$

The upper sign in the right side of Eq. (11) corresponds to the direct modal ray, which has no turning points between the source and receiver, and the lower sign corresponds to a modal ray with a turning point. In the special case of sound propagation along shore, $H_s = H_r$ and only rays with turning points connect such points. In this case, the travel time is twice the time of propagation to the turning point:

$$T_n = 2H_s \cos\gamma_n \frac{\left|\cos\psi\right| \cot\alpha}{\left(1 - \cos^2\gamma_n \sin^2\psi\right) c} = 2H_s \frac{\left|\cos\psi\right| \cot\alpha}{\left(1 - \cos^2\gamma_n \sin^2\psi\right) c_n(\omega, H_s)}. \tag{13}$$

Using Eqs. (6) and (12), it is easy to verify that Eq. (11) reduces to Eqs. (5) and (8) when $\sin\psi = 0$.

3. Effects of the seafloor slope on normal mode dispersion

In application to shallow-water acoustic waveguides, time-warping transform allows one to separate contributions of individual normal modes into acoustic field and retrieve modal dispersion curves without using hydrophone arrays [1–4]. "Warped time," t_w, and signal frequency in the warped domain, f_w, are given by the equations (e.g., [1, 2])

$$t_w = \sqrt{t^2 - t_r^2}, \quad f_w = f(t)\sqrt{1 - t_r^2/t^2}. \tag{14}$$

Here t_r and $f(t)$ are a reference travel time and the instantaneous frequency of the signal arriving at the receiver at time t. In a range-independent waveguide with a uniform water column, reference travel time $t_r = r/c$, where r is range, i.e., source-receiver horizontal separation. If the dispersion curve of a normal mode is found in physical domain, Eq. (14) map the dispersion curve into the warped domain, and vice versa.

According to Eq. (6), application of the transform (14) to range-independent waveguides with ideal (i.e., pressure-release and rigid) boundaries gives $f_w = F_n$ for all values of t_w, $0 < t_w < \infty$, where F_n is the cut-off frequency of the normal mode. Hence, spectrograms of all normal modes are straight lines $f_w = F_n$ in the warped domain.

3.1 Time-warping in range-dependent waveguides

Range-dependence of a waveguide has an effect on dispersion curves in the warped domain. In geo-acoustic inversions, this effect can be misinterpreted as the effect of ocean bottom stratification. As a first step towards understanding and quantifying the manifestations of the range-dependence in the warped domain, here we illustrate the effect of bottom slope for the simple case of an ideal wedge.

When source-receiver horizontal separation is r, the minimum travel time in the ideal wedge equals r/c, see Eq. (6). We choose the minimum travel time, r/c, as the reference travel time t_r in Eq. (14) in applications of the warping transform to the ideal wedge. Then, the warped travel time t_w and warped frequency f_w are always real and non-negative.

Figure 1 illustrates the dependence between frequency and travel time at up- and downslope propagation in an ideal wedge. In this example, water depths at the source and receiver points differ by the factor of 2 (strong range dependence). The figure clearly shows systematic deviations of the dispersion curves from those in a range-independent waveguide with the same average depth. The warped frequencies of individual normal modes are no longer constant and steadily increase with the warped travel time. The warped frequencies are higher than in a range-independent waveguide with the same average depth. Note that wave frequency and warped frequency scale with depth. Mode travel times and warped travel times scale as cotα; other than that, the graphs shown in Fig. 1 are unaffected by the bottom slope. This is also the case at sound propagation in the penetrable wedge (Fig. 2).

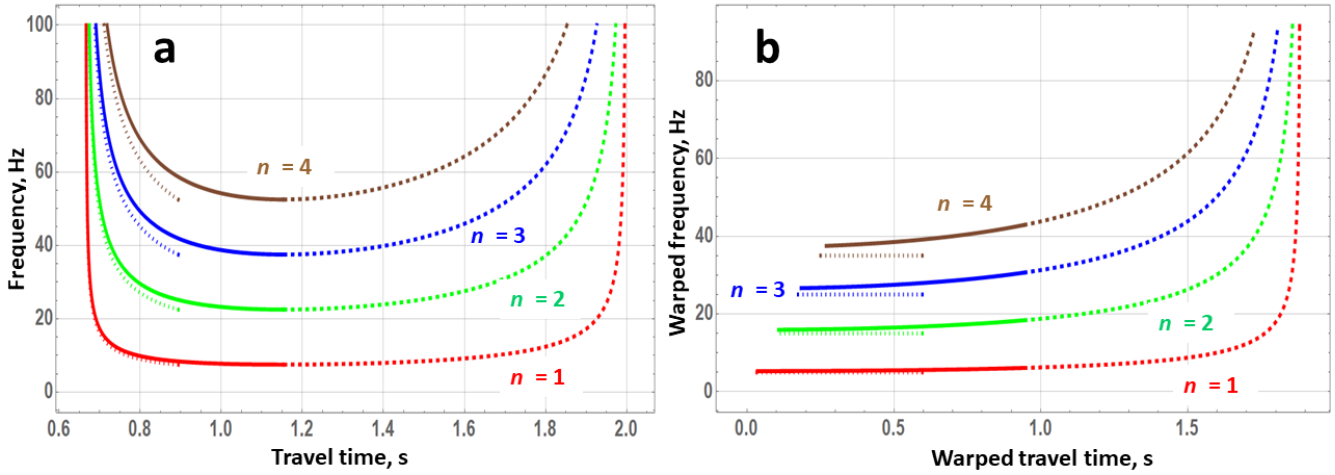

Figure 1: Adiabatic normal mode travel times in a coastal wedge with pressure-release surface and rigid bottom. Dispersion curves of the first four normal modes are shown in the physical (a) and warped (b) domains. Source and receiver are located at depths 100 m and 50 m on a line perpendicular to the coastline. Sound speed in water is 1500 m/s, seafloor slope is 0.05 rad ≈ 2.86°. Solid and dashed lines refer, respectively, to direct up- or downslope propagation between the source and receiver and to modes propagating downslope after reflection from their respective mode cut-offs at shallower depths. Mode travel times over the same range in a range-independent waveguide with the same average depth of 75 m are shown by dotted lines.

Under conditions of applicability of the adiabatic approximation, a normal mode propagating upslope radiates all its energy into the bottom in the vicinity of the mode's cutoff in the penetrable wedge [6]. In contrast to the ideal wedge, there is no reflection from the cutoff. For any normal mode, travel times between depths $H_1 < H_2$ are, of course, the same, whether the mode propagates up- or downslope. The dependence of mode travel time on the mode order n and wave frequency is given by Eqs. (1) and (5) and is illustrated in Fig. 2 for a waveguide with a fluid bottom. In Fig. 2, we assume that the source radiates sound in the 10–150 Hz frequency band.

The most apparent difference between the dispersion curves in the penetrable wedge and in a range-independent waveguide with the same average depth (dashed lines) is the disappearance (for modes n = 2, 3, 4) or contraction (for mode 1) of the anomalous dispersion part of the curves (Fig. 2). In addition, at normal dispersion, instantaneous frequencies tend to be higher, at a given travel time, in the wedge than in the Pekeris waveguide. Another notable difference from the range-independent case is the decrease in the maximum travel time (Fig. 2a). This can be attributed to the minimum group speed occurring at different frequencies at different depths, so that at all frequencies only a small portion of the entire up- or downslope propagation path is covered at near-minimum group speeds. In the warped domain, contraction of the frequency range or complete disappearance of the anomalous dispersion gives the warping results in the penetrable wedge (Fig. 2b) a much closer resemblance of the results in the range-independent ideal waveguide than in the case of the Pekeris waveguide.

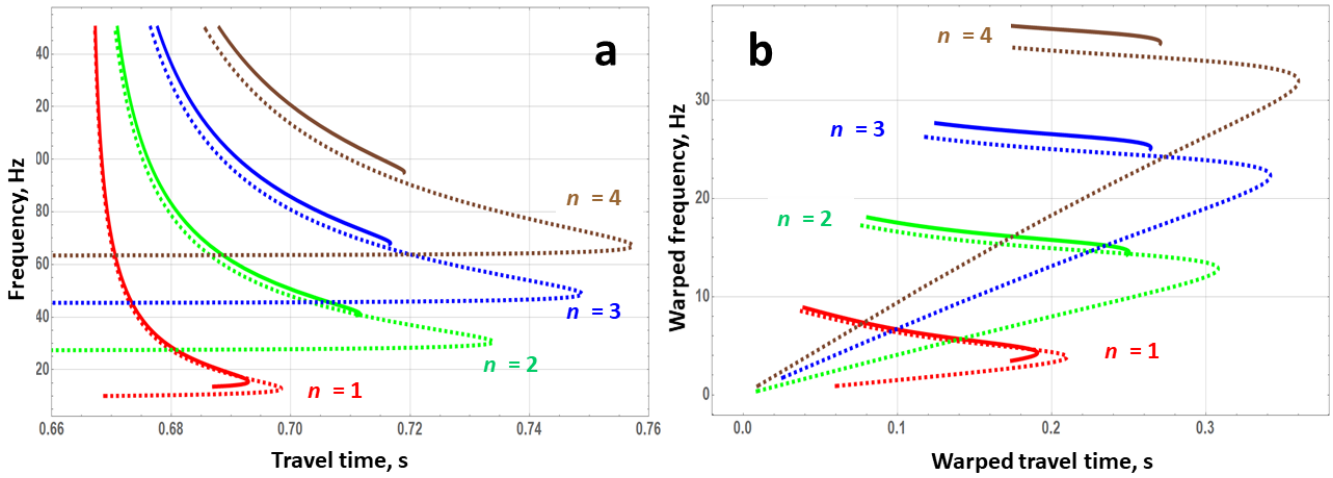

Figure 2: Dispersion curves of the first four adiabatic normal modes in the physical (a) and warped (b) domains at upslope or downslope propagation in a penetrable wedge with a fluid bottom. Source and receiver depths are 50 m and 100 m. Sound speeds in the water column and bottom are c =1500 m/s and c_b =1800 m/s, respectively; the ratio of bottom and water densities m = 2.2. Dashed lines show dispersion curves of normal modes in a range-independent waveguide with the same water and bottom parameters and depth of 75 m, at the same propagation range of 999.167 m.

3.2 Manifestations of horizontal refraction in the warped domain

Seafloor slope has a significant effect on mode dispersion in a penetrable wedge even when the water depths at the source and receiver locations are the same. In this case of cross-slope propagation the effect is due to horizontal refraction [6, 7]. Unlike the perfect wedge (Section 2.3), no closed-form analytical solutions are available for horizontal (modal) eigenrays in a penetrable wedge. The right-most hand side in Eq. (10) gives a convenient expression for calculating the travel time on a modal ray.

Figure 3 illustrates modal dispersion at cross-range propagation. Normal modes in a wedge experience stronger dispersion than at propagation over the same range in the range-independent (Pekeris) waveguide with the same physical parameters (Fig. 3a). This leads to an increase of the received signal duration. In particular, for a fixed frequency range in the normal dispersion band, the maximum travel time is greatly increased compared to the Pekeris waveguide. Lower frequencies are responsible for later arrivals and are more sensitive to the seafloor slope (Fig. 3a). In contrast, travel times at higher frequencies, where the value of the group speed approaches the sound speed in water, are insensitive to the slope. Figure 3a indicates that the minimum effective group speed occurs (i.e., the adiabatic mode travel time reaches its maximum as a function of frequency) at a higher frequency at cross-slope propagation than in the Pekeris waveguide. At all frequencies considered, sound propagates slower in the wedge than in

the Pekeris waveguide. This should be contrasted with the *decrease* in mode phase Φ_n due to horizontal refraction [8].

In the warped domain, horizontal refraction manifests itself in increasing modal travel time and values of the warped frequency (Fig. 3b). There is also a qualitative change in the dispersion curves of modes 2–4 in the warped domain. Unlike the Pekeris waveguide and the case of upslope/downslope propagation (Fig. 2b), warped frequency increases with increasing warped time. As a result, the dispersion curves in the warped domain start to resemble the dispersion curves in the ideal waveguide rather than in the Pekeris waveguide.

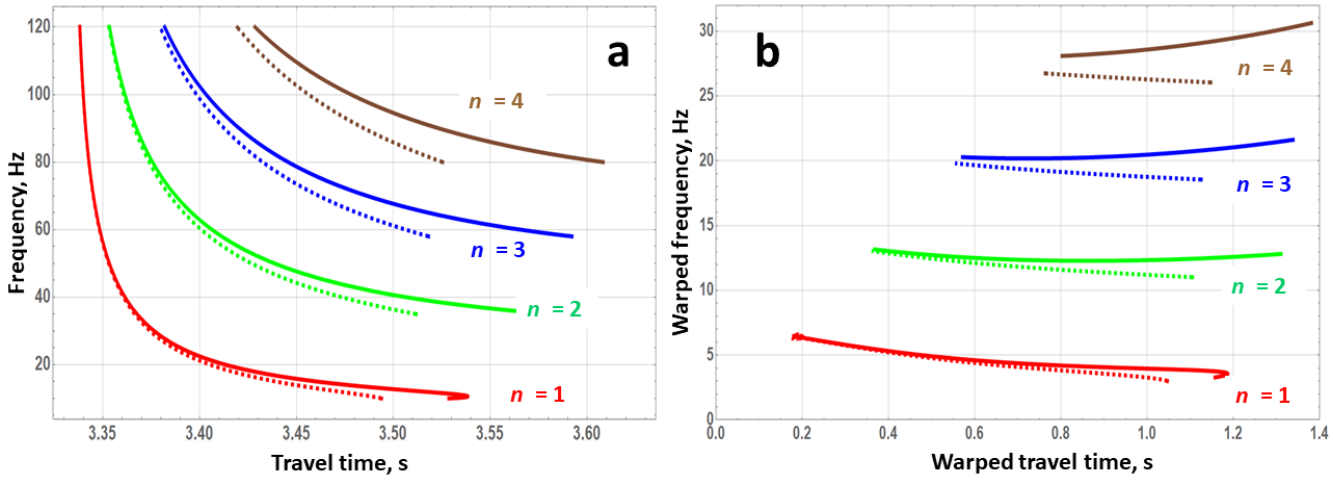

Figure 3: Dispersion curves of the first four adiabatic normal modes in the physical (a) and warped (b) domains at cross-slope propagation in a penetrable wedge with a fluid bottom. Source and receiver depths are 100 m. Sound speeds in the water column and bottom are c =1500 m/s and c_b =1800 m/s, respectively; density ratio m = 2.2. Dashed lines show dispersion curves of normal modes in a range-independent Pekeris waveguide with the same water and bottom parameters and depth of 75 m, at the same propagation range of 5000 m. The dispersion curves are shown in the frequency bands 10–120, 35–120, 58–120, and 80–120 Hz for modes 1, 2, 3, and 4, respectively.

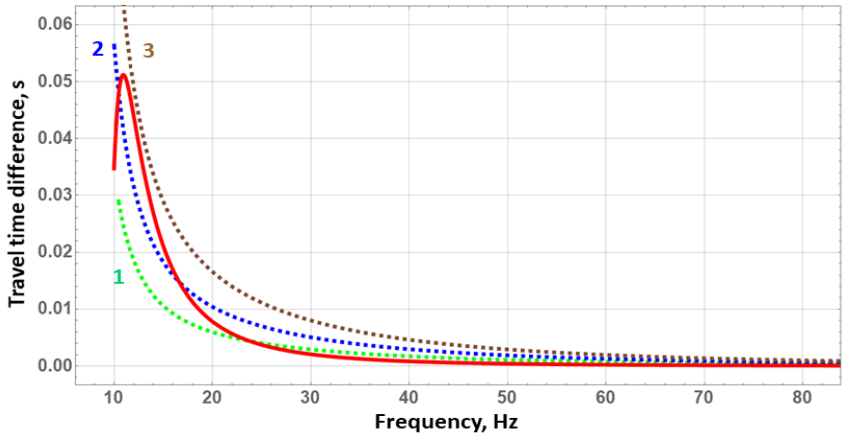

Figure 4: Comparison of the effects of cross-slope propagation and bottom sound speed on mode dispersion curves. Solid line shows the travel time of mode 1 at cross-slope propagation in a penetrable wedge with seafloor slope of 0.05 rad and bottom sound speed c_b = 1800 m/s. Dashed lines show travel times of mode 1 in Pekeris waveguides with three different bottom sound speed values: c_b = 1900 m/s (1), 2000 m/s (2), and 2200 m/s (3).

Propagation range r = 5000 m, water depth H = 100 m, sound speed in water c = 1500 m/s; the ratio of bottom and water densities m = 2.2. The travel time of mode 1 in the Pekeris waveguide with c_b = 1800 m/s is subtracted from the mode travel times in the figure.

The increase in the mode dispersion and maximum modal travel time due to horizontal refraction may have important implications for geoacoustic inversions. Although analysis of any inverse problems is beyond the scope of this paper, we emphasize that disregard of horizontal refraction due to bottom slopes of a few degrees can lead to a positive bias in the inverted bottom sound speed. The errors in the inversion results for the bottom sound speed can easily reach hundreds of meters per second. This is illustrated in Fig. 4, where mode 1 travel time at cross-slope propagation is compared to travel times in the Pekeris waveguides with different bottom sound speeds. In this example, c_b = 1800 m/s in the penetrable wedge but one needs bottom sound speeds between 1900 and 2200 m/s to match long travel times at low frequencies, where horizontal refraction is most pronounced. Due to bottom slope, the travel times increase by up to 45 ms and 85 ms for modes 1 and 4, respectively (Fig. 3a). The best match by a range-independent geoacoustic model exaggerates the actual c_b by ~200 m/s (Fig. 4).

4. Conclusion

Using simple models of the coastal ocean, we have found that the seafloor slope changes mode dispersion in a way conducive to mode separation by application of the time-warping transform. However, ignoring even moderate seafloor slopes in geoacoustic inversions can lead to unexpectedly large errors in the estimates of sound speed in the bottom.

Analysis presented in the paper will be extended in the conference presentation to more general environments using a perturbation theory and numerical techniques.

This work has been supported by NSF, grant OCE1657430; BSF, grant 2016545; and ONR, award N00014-19-WX-00462.

REFERENCES

1 Bonnel, J., and Chapman, N. R. Geoacoustic inversion in a dispersive waveguide using warping operators, *Journal of the Acoustical Society of America,* **130**, EL101–EL107, (2011).

2 Bonnel, J., Dosso, S. E., and Chapman, N. R. Bayesian geoacoustic inversion of single hydrophone light bulb data using warping dispersion analysis, *Journal of the Acoustical Society of America,* **134**, 120–130, (2013).

3 Bonnel, J., Lin, Y.-T., Eleftherakis, D., Goff, J. A., Dosso, S., Chapman, R., Miller, J. H., and Potty, G. R. Geoacoustic inversion on the New England Mud Patch using warping and dispersion curves of high-order modes, *Journal of the Acoustical Society of America,* **130**, EL405–EL411, (2018).

4 Sergeev, S. N., Shurup, A. S., Godin, O. A., Vedenev, A. I., Goncharov, V. V., Mukhanov, P. Yu., Zabotin, N. A., and Brown, M. G. Separation of acoustic normal modes in the Florida Straits using noise interferometry, *Acoustical Physics,* **63** (1), 76–85, (2017).

5 Brekhovskikh, L. M., and Godin, O. A. *Acoustics of Layered Media. 1: Plane and Quasi-Plane Waves*. 2nd edn., Springer, Berlin (1998). Secs. 2.2, 4.2.

6 Brekhovskikh, L. M., and Godin, O. A. *Acoustics of Layered Media. 2 Point Sources and Bounded Beams*. 2nd edn., Springer, Berlin (1999). Secs. 4.5, 7.4.

7 Harrison, C. H. Acoustic shadow zones in the horizontal plane, *Journal of the Acoustical Society of America,* **65** (1), 56–61, (1979).

8 Godin, O. A. A 2-D description of sound propagation in a horizontally-inhomogeneous ocean, *Journal of Computational Acoustics,* **10**, 123–151, (2002).